

Semiclassical truncated-Wigner-approximation theory of molecular-vibration-polariton dynamics in optical cavities

Nguyen Thanh Phuc*

Department of Molecular Engineering, Graduate School of Engineering, Kyoto University, Kyoto 615-8510, Japan

It has been experimentally demonstrated that molecular-vibration polaritons formed by strong coupling of a molecular vibration to an infrared cavity mode can significantly modify the physical properties and chemical reactivity of various molecular systems. However, a complete theoretical understanding of the underlying mechanisms of the modifications remains elusive due to the complexity of the hybrid system, especially the collective nature of polaritonic states in systems containing many molecules. We develop here the semiclassical theory of molecular-vibration-polariton dynamics based on the truncated Wigner approximation that is tractable in large molecular systems and simultaneously captures the quantum character of photons in the optical cavity. The theory is then applied to investigate the nuclear dynamics of a system of identical diatomic molecules having the ground-state Morse potential and strongly coupled to an infrared cavity mode in the ultrastrong coupling regime. The collective and resonance effects of the molecular-vibration-polariton formation on the nuclear dynamics are observed.

Keywords: truncated Wigner approximation, molecular-vibration polariton, light-matter coupling, optical cavity

Introduction—Strongly coupling a molecular-vibration mode to an infrared cavity mode results in the formation of molecular-vibration polaritons—hybrid states with both light and matter characters. Numerous experiments have demonstrated that strong light-matter coupling can significantly modify the physical properties and chemical reactivity of molecular systems [1–3]. Examples include the acceleration or hindrance of the chemical reactivity of molecules [4–10], chemoselectivity [11], supramolecular assembly and crystallization [12, 13], vibrational energy transfer [14], ferromagnetism, and superconductivity [15, 16]. Despite great efforts [17–28], the mechanisms underlying changes to molecular properties and reactivity from strong vibrational coupling remain unclear [29–32]. The collective effect of molecular-polariton formation on chemical reactivity is a topic of debate. The issue arises from the conflict between the non-locality of light-matter coupling and the locality of chemical reactions. Performing a fully quantum mechanical simulation of molecular dynamics is prohibitively expensive for large systems containing many molecules.

On the other hand, it is possible for strong light-matter coupling to occur even in the absence of light due to the quantum nature of the electromagnetic field. The optical mode has zero-point energy, which results in vacuum fluctuations. In this work, we develop a semiclassical theory of molecular-vibration-polariton dynamics that captures the quantum character of photons in the optical cavity. This theory is applicable to large molecular systems. It is based on the truncated Wigner approximation (TWA), in which the equation of motion for the Wigner function in the phase-space representation is truncated at the leading order of the expansion with respect to the parame-

ter characterizing the quantum fluctuation [33–35]. The leading-order equation of motion is unaffected by quantum fluctuations, which are only reflected in the Wigner distribution of the initial state. In other words, in the TWA, the Heisenberg uncertainty principle for the quantum fluctuations is satisfied, while the equation of motion of physical observables in the phase space takes the classical form. The TWA has been developed using quantum coherent states for applications in quantum optics and bosonic cold atoms [36, 37] and using the coordinate-momentum representation in the context of quantum dynamics [34, 38]. In this work, we combine the coherent-state and coordinate-momentum representations to develop the TWA for strongly coupled molecule-cavity systems. The developed theory is then applied to investigate the nuclear dynamics of a system of identical diatomic molecules. These molecules have a ground-state Morse potential and a nonlinear electric dipole moment [39], and they are strongly coupled to an infrared cavity mode in the ultrastrong coupling regime [40]. The comparison of the semiclassical dynamics obtained by the TWA with the fully quantum mechanical dynamics obtained by solving the quantum master equation for the single-molecule system confirms the validity of TWA. For a system of many molecules, all aligned parallel to the polarization direction of the cavity mode, the dynamic amplitude of nuclear displacement does not decrease with the increasing number of molecules, provided that the collective coupling strength is kept constant. This implies that, unlike linear systems such as a group of harmonic oscillators linearly coupled to an optical cavity, the collective effect can be observed in the molecular-vibration-polariton dynamics of nonlinear systems such as those with the Morse potential. The resonance effect of the molecular-vibration-polariton formation is also observed, as the dynamic amplitude of nuclear displacement is maximum when the cavity frequency is resonant with

*Electronic address: nthanhpuc@moleng.kyoto-u.ac.jp

the energy spacing between the vibrational ground state and the first excited state of the Morse potential. Using the TWA, the dependence of the molecular nuclear dynamics on the cavity loss rate is investigated. Finally, by investigating the molecular-vibration-polariton dynamics in a system of molecules with random orientations, it is found that the collective effect persists if the system and the observables are nonlinear.

TWA theory of molecular-vibration-polariton dynamics– As illustrated in Fig. 1, consider a system of N molecules strongly coupled to an optical cavity mode whose frequency ω_c is in the infrared region so that the electronic excitations of the molecules can be ignored. The dipole-gauge total Hamiltonian of the system $\hat{H} = \hat{H}_m + \hat{H}_c$ is obtained by performing the Power-Zienau-Woolley gauge transformation on the minimal coupling QED Hamiltonian in the Coulomb gauge [41–43]. The nuclear dynamics on the electronic-ground-state potential energy surface of the molecules are represented by the molecular Hamiltonian

$$\hat{H}_m = \sum_{n=1}^N \left[\sum_{j \in n} \frac{\hat{\mathbf{P}}_{nj}^2}{2M_{nj}} + \hat{V}_g^{(n)} \right] + \sum_{n=1}^N \sum_{l > n} \hat{V}_{\text{int}}^{(nl)}, \quad (1)$$

where $\hat{\mathbf{P}}_{nj}$ denotes the momentum operator of the j th nuclear degree of freedom in the n th molecule with the effective mass M_{nj} , $\hat{V}_g^{(n)}$ represents the electronic-ground-state potential energy of the n th molecule, and $\hat{V}_{\text{int}}^{(nl)}$ is the interaction between the n th and l th molecules. The cavity photon energy and the molecule-cavity coupling are included in the Hamiltonian

$$\begin{aligned} \hat{H}_c = & \hbar\omega_c \left(\hat{a}^\dagger \hat{a} + \frac{1}{2} \right) + i\omega_c \left(\sum_{n=1}^N \hat{\boldsymbol{\mu}}_n \cdot \mathbf{A}_0 \right) (\hat{a}^\dagger - \hat{a}) \\ & + \frac{\omega_c}{\hbar} \left(\sum_{n=1}^N \hat{\boldsymbol{\mu}}_n \cdot \mathbf{A}_0 \right)^2, \end{aligned} \quad (2)$$

where \hat{a} denotes the annihilation operator of a cavity photon, $\mathbf{A}_0 = \sqrt{\frac{\hbar}{2\omega_c \epsilon \mathcal{V}}} \hat{\mathbf{e}}$ is the vector potential amplitude of the cavity field (with ϵ , \mathcal{V} , and $\hat{\mathbf{e}}$ being the permittivity inside the cavity, effective cavity quantization volume, and unit vector of the cavity field polarization direction, respectively), and $\hat{\boldsymbol{\mu}}_n$ represents the electric dipole moment operator of the n th molecule in its electronic ground state. The dipole self-energy, which is the last term in Eq. (2), cannot be neglected in the ultrastrong coupling regime [40, 44].

The cavity loss is caused by the coupling between the optical mode inside the cavity and the electromagnetic field environment outside the cavity. The Lindblad quantum master equation for the density operator $\hat{\rho}$ describes the effect of cavity dissipation on the system dynamics under the Markov approximation [36, 45]:

$$\frac{d\hat{\rho}}{dt} = -\frac{i}{\hbar} [\hat{H}, \hat{\rho}] + \mathcal{L}_c \hat{\rho}. \quad (3)$$

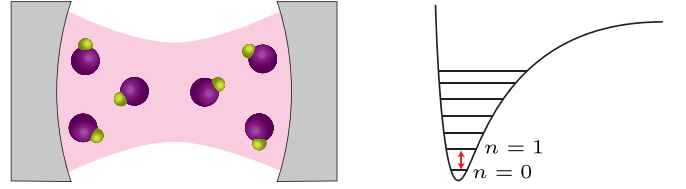


FIG. 1: Schematic illustration of a system of diatomic molecules whose nuclear motions are strongly coupled to an infrared cavity mode (light magenta) of an optical resonator. The molecular ground-state potential is modeled by the anharmonic Morse potential, and the cavity frequency is in close resonance with the energy difference between the vibrational ground state ($n = 0$) and the first excited state ($n = 1$).

Here, the decay of the cavity field at the rate κ is accounted for by the Liouville superoperator \mathcal{L}_c whose action on the density operator is given by

$$\begin{aligned} \mathcal{L}_c \hat{\rho} = & \kappa (\bar{n} + 1) (2\hat{a}\hat{\rho}\hat{a}^\dagger - \hat{a}^\dagger\hat{a}\hat{\rho} - \hat{\rho}\hat{a}^\dagger\hat{a}) \\ & + \kappa \bar{n} (2\hat{a}^\dagger\hat{\rho}\hat{a} - \hat{a}\hat{a}^\dagger\hat{\rho} - \hat{\rho}\hat{a}\hat{a}^\dagger), \end{aligned} \quad (4)$$

where $\bar{n} = 1/(e^{\hbar\omega_c/(k_B T)} - 1)$ is the average number of photons with frequency ω_c in the environment at temperature T .

To derive the semiclassical TWA theory for molecular-vibration-polariton dynamics, the Wigner quasiprobability distribution function is defined in the joint phase space of molecular nuclear motion and cavity field. The Wigner function for the density operator $\hat{\rho}$ and the Weyl symbol of an arbitrary operator $\hat{\Omega}$ are defined by

$$\begin{aligned} W(\mathbf{R}, \mathbf{P}, \alpha) = & \frac{1}{2} \int d\boldsymbol{\xi} \iint d\boldsymbol{\eta}^* d\boldsymbol{\eta} \\ & \times e^{i\mathbf{P} \cdot \boldsymbol{\xi} / \hbar} e^{-|\alpha|^2 - |\boldsymbol{\eta}|^2 / 4} e^{\boldsymbol{\eta}^* \alpha - \boldsymbol{\eta} \alpha^*} \\ & \times \left\langle \mathbf{R} - \frac{\boldsymbol{\xi}}{2}, \alpha - \frac{\boldsymbol{\eta}}{2} \left| \hat{\rho} \right| \mathbf{R} + \frac{\boldsymbol{\xi}}{2}, \alpha + \frac{\boldsymbol{\eta}}{2} \right\rangle \end{aligned} \quad (5)$$

and

$$\begin{aligned} \Omega_W(\mathbf{R}, \mathbf{P}, \alpha) = & \frac{1}{2} \int d\boldsymbol{\xi} \iint d\boldsymbol{\eta}^* d\boldsymbol{\eta} \\ & \times e^{i\mathbf{P} \cdot \boldsymbol{\xi} / \hbar} e^{-|\alpha|^2 - |\boldsymbol{\eta}|^2 / 4} e^{\boldsymbol{\eta}^* \alpha - \boldsymbol{\eta} \alpha^*} \\ & \times \left\langle \mathbf{R} - \frac{\boldsymbol{\xi}}{2}, \alpha - \frac{\boldsymbol{\eta}}{2} \left| \hat{\Omega} \right| \mathbf{R} + \frac{\boldsymbol{\xi}}{2}, \alpha + \frac{\boldsymbol{\eta}}{2} \right\rangle, \end{aligned} \quad (6)$$

respectively, where $\mathbf{R} = \{\mathbf{R}_{nj}\}$, $\mathbf{P} = \{\mathbf{P}_{nj}\}$, and $\boldsymbol{\xi} = \{\boldsymbol{\xi}_{nj}\}$ denote the sets of coordinate and momentum variables for all the nuclear degrees of freedom of the molecules inside the cavity, and the integration measure is defined as $d\boldsymbol{\eta}^* d\boldsymbol{\eta} = d\text{Re}\boldsymbol{\eta} d\text{Im}\boldsymbol{\eta} / \pi$. Here, $|\mathbf{R}, \alpha\rangle = |\mathbf{R}\rangle \otimes |\alpha\rangle$ is the tensor product of the molecular coordinate eigenstate with the eigenvalue \mathbf{R} and the photonic coherent state with the amplitude α . The Weyl symbol of the product $\hat{\Omega} = \hat{\Omega}_1 \hat{\Omega}_2$ of two operators can

be obtained by using the Moyal product [35]:

$$\Omega_W = \Omega_{1W} \exp\left(\frac{\Lambda_c - i\hbar\Lambda}{2}\right) \Omega_{2W}, \quad (7)$$

where

$$\Lambda = \frac{\overleftarrow{\partial}}{\partial \mathbf{P}} \cdot \frac{\overrightarrow{\partial}}{\partial \mathbf{R}} - \frac{\overleftarrow{\partial}}{\partial \mathbf{R}} \cdot \frac{\overrightarrow{\partial}}{\partial \mathbf{P}}, \quad (8)$$

$$\Lambda_c = \frac{\overleftarrow{\partial}}{\partial \alpha} \frac{\overrightarrow{\partial}}{\partial \alpha^*} - \frac{\overleftarrow{\partial}}{\partial \alpha^*} \frac{\overrightarrow{\partial}}{\partial \alpha}. \quad (9)$$

Here, the left (right) arrow implies that the derivative acts on the operator on the left (right). Similarly, the Weyl symbol of the commutator $\hat{\Omega} = [\hat{\Omega}_1, \hat{\Omega}_2]$ of two operators can be obtained by using the Moyal bracket:

$$\Omega_W = 2\Omega_{1W} \sinh\left(\frac{\Lambda_c - i\hbar\Lambda}{2}\right) \Omega_{2W}. \quad (10)$$

The quantum master equation (3) then translates into a partial differential equation for the Wigner function. By dropping all terms containing higher-than-second-order derivatives, the obtained equation for the Wigner function is found to be

$$\begin{aligned} \frac{\partial W}{\partial t} = & \sum_{n=1}^N \sum_{j \in n} \left[-\frac{\mathbf{P}_{nj}}{M_{nj}} \cdot \frac{\partial W}{\partial \mathbf{R}_{nj}} + \left(\frac{\partial V_g^{(n)}}{\partial \mathbf{R}_{nj}} + \sum_{l \neq n} \frac{\partial V_{\text{int}}^{(nl)}}{\partial \mathbf{R}_{nj}} \right) \right. \\ & \cdot \frac{\partial W}{\partial \mathbf{P}_{nj}} \left. \right] - i\omega_c \left[\frac{\partial(\alpha^* W)}{\partial \alpha^*} - \frac{\partial(\alpha W)}{\partial \alpha} \right] - \frac{\omega_c}{\hbar} \sum_{n=1}^N \\ & \left[(\boldsymbol{\mu}_n \cdot \mathbf{A}_0) \left(\frac{\partial W}{\partial \alpha^*} + \frac{\partial W}{\partial \alpha} \right) + i\hbar(\alpha - \alpha^*) \sum_{j \in n} \right. \\ & \left. \sum_{\lambda, \nu=x, y, z} \frac{\partial \mu_n^\lambda}{\partial R_{nj}^\nu} A_0^\lambda \frac{\partial W}{\partial P_{nj}^\nu} \right] + \frac{2\omega_c}{\hbar} \left(\sum_{n=1}^N \boldsymbol{\mu}_n \cdot \mathbf{A}_0 \right) \\ & \times \sum_{n=1}^N \sum_{j \in n} \sum_{\lambda, \nu=x, y, z} \frac{\partial \mu_n^\lambda}{\partial R_{nj}^\nu} A_0^\lambda \frac{\partial W}{\partial P_{nj}^\nu} + \kappa \left[\frac{\partial(\alpha^* W)}{\partial \alpha^*} \right. \\ & \left. + \frac{\partial(\alpha W)}{\partial \alpha} + (2\bar{n} + 1) \frac{\partial^2 W}{\partial \alpha \partial \alpha^*} \right]. \quad (11) \end{aligned}$$

Note that a general Fokker-Planck equation $\partial P / \partial t = \left[-\sum_j \partial A_j / \partial x_j + (1/2) \sum_{i,j} \partial^2 D_{ij} / \partial x_i \partial x_j \right] P$ for a distribution function $P(\mathbf{x}, t)$ with a positive definite diffusion matrix $D_{ij}(\mathbf{x})$ is equivalent to the Ito stochastic differential equation $d\mathbf{x}_t = \mathbf{A}(\mathbf{x}_t)dt + \mathbf{B}(\mathbf{x}_t)d\mathbf{W}_t$, where $\mathbf{A}(\mathbf{x})$ is the column vector of the drifts $A_j(\mathbf{x})$, the matrix $\mathbf{B}(\mathbf{x})$ is defined by the factorization $\mathbf{D}(\mathbf{x}) = \mathbf{B}(\mathbf{x})\mathbf{B}(\mathbf{x})^T$, and \mathbf{W}_t is a column vector of independent Wiener processes [36, 46]. From Eq. (11), the stochastic differential equation for the coupled molecule-cavity system is given

by

$$d\mathbf{R}_{nj} = \frac{\mathbf{P}_{nj}}{M_{nj}} dt, \quad (12)$$

$$\begin{aligned} dP_{nj}^\nu = & \left\{ -\left(\frac{\partial V_g^{(n)}}{\partial R_{nj}^\nu} + \sum_{l \neq n} \frac{\partial V_{\text{int}}^{(nl)}}{\partial R_{nj}^\nu} \right) - \frac{\omega_c}{\hbar} \left[i\hbar(\alpha^* - \alpha) \right. \right. \\ & \left. \left. + 2 \sum_{n=1}^N \boldsymbol{\mu}_n \cdot \mathbf{A}_0 \right] \frac{\partial \mu_n^\lambda}{\partial R_{nj}^\nu} A_0^\lambda \right\} dt, \quad (13) \end{aligned}$$

$$d\alpha = \left[(-i\omega_c - \kappa)\alpha + \frac{\omega_c}{\hbar} \sum_{n=1}^N \boldsymbol{\mu}_n \cdot \mathbf{A}_0 \right] dt + dA, \quad (14)$$

where dA represents a complex-number stochastic process with $dA = dA_r + i dA_i$ and $dA_{r,i} = \sqrt{\kappa(\bar{n} + 1/2)} dW_{r,i}$. Here, $dW_{r,i}$ are independent Wiener processes, i.e., $dW_{r,i} = \Theta_{r,i} dt$ and $\Theta_{r,i}$ are white noises: $\langle \Theta_{r,i}(t) \rangle = 0$, $\langle \Theta_{r,i}(t) \Theta_{r,i}(t') \rangle = \delta(t - t')$. Apart from the decaying and stochastic terms in the last equation, Eqs. (12)-(14) have the same form as the classical equations of motions for the dynamic variables \mathbf{R} , \mathbf{P} , and α [20]. To the leading order in quantum fluctuation, the expectation value of an arbitrary operator $\hat{\Omega}$ in the coupled molecule-cavity system is given under the TWA by

$$\begin{aligned} \langle \hat{\Omega} \rangle \simeq & \iint d\mathbf{R}_0 d\mathbf{P}_0 \iint d\alpha_0^* d\alpha_0 W_0(\mathbf{R}_0, \mathbf{P}_0, \alpha_0) \\ & \times \Omega_W(\mathbf{R}(t), \mathbf{P}(t), \alpha(t)). \quad (15) \end{aligned}$$

Here, W_0 is the Wigner function for the initial density operator $\hat{\rho}(t=0)$, Ω_W is the Weyl symbol of the operator $\hat{\Omega}$, and $\mathbf{R}(t)$, $\mathbf{P}(t)$, and $\alpha(t)$ represent the values of the dynamic variables at time t obtained by solving the set of equations of motion (12)-(14) along with the set of initial conditions: $\mathbf{R}(t=0) = \mathbf{R}_0$, $\mathbf{P}(t=0) = \mathbf{P}_0$, and $\alpha(t=0) = \alpha_0$.

Molecular-vibration-polariton dynamics in a system of diatomic molecules— We now apply the above-developed TWA theory to investigate the molecular-vibration-polariton dynamics in a system of identical diatomic molecules. The vibration of a molecule in its electronic ground state is modeled by the Morse potential:

$$V_g(q) = D \left(1 - e^{-\alpha(q - q_e)} \right)^2. \quad (16)$$

Here, q represents the distance between the two nuclei, and q_e and D denote the equilibrium bond length and the dissociation energy, respectively. The system is assumed to be sufficiently dilute that the inter-molecular interactions are negligible. The functional form assumed for the dipole moment function of a diatomic molecule is given by

$$\mu(q) = A q e^{-Bq^4}. \quad (17)$$

In the numerical calculations below, the parameters for the HF molecule will be used: $\alpha = 1.174$, $D = 0.225$,

$q_e = 1.7329$, $A = 0.4541$, and $B = 0.0064$ [39]. The reduced mass for the relative motion of the two nuclei is $M = 1744.59$. These values are all given in atomic units.

Suppose that each molecule is initially prepared in the ground state of the Morse potential while the optical cavity is initially in the vacuum state before they start to couple with each other. The Wigner function of the total system at $t = 0$ is then given by the product of molecular and photonic Wigner functions. The molecular Wigner function for the ground state $|\psi_0\rangle$ of the Morse potential is calculated to be [47]

$$\begin{aligned} W_m(q, p) &= \int_{-\infty}^{\infty} d\xi \psi_0^* \left(q + \frac{\xi}{2} \right) \psi_0 \left(q - \frac{\xi}{2} \right) e^{ip\xi/\hbar} \\ &= \frac{4(2\lambda - 1)}{\Gamma(2\lambda)} \left(2\lambda e^{-\alpha(q - q_e)} \right)^{2\lambda - 1} \\ &\quad \times K_{2ip/(\hbar\alpha)} \left(2\lambda e^{-\alpha(q - q_e)} \right), \end{aligned} \quad (18)$$

where $\lambda = \sqrt{2MD}/\alpha\hbar$, $\Gamma(z) = \int_0^\infty dt t^{z-1} e^{-t}$ is the gamma function, and $K_\nu(\xi) = (1/2) \int_0^\infty dx x^{\nu-1} \exp[-(\xi/2)(x + 1/x)]$ is the modified Bessel function of the third kind. By making a variable transformation $u = \ln x$, the modified Bessel function can be rewritten as $K_\nu(\xi) = (1/2) \int_{-\infty}^{\infty} du \exp(\nu u - \xi \cosh u)$ and calculated numerically using, for example, the Simpson's 1/3 formula [48]. The photonic Wigner function for the vacuum state of cavity photons is given by $W_c = (2/\pi) e^{-2|\alpha|^2}$. An ensemble of initial values of q , p , and α following the Wigner distribution functions is created using the Monte Carlo M(RT)² algorithm [49]. The Weyl symbol of the molecular nuclear operator \hat{q} is q , while that of the cavity photon number $\hat{n} = \hat{a}^\dagger \hat{a}$ is given by $n_W = |\alpha|^2 - 1/2$.

In the numerical calculations below, the molecule-cavity collective coupling strength is set to $g\sqrt{N}A\sqrt{\frac{\hbar}{M\omega_0}} = 0.1\hbar\omega_c$, corresponding to the ultrastrong coupling regime [40]. Here, $g = |\mathbf{A}_0|\omega_c$ characterizes the light-matter coupling strength, $\omega_0 = \alpha\sqrt{2D/M}$ is the harmonic-oscillator frequency at the equilibrium point of the Morse potential, and $\sqrt{\frac{\hbar}{M\omega_0}}$ is the characteristic length scale of a harmonic oscillator with frequency ω_0 . As a result of the ultrastrong coupling, both the molecular nuclei and cavity photons would evolve with time, even if they are initially prepared in their ground states. The cavity frequency ω_c is chosen to be resonant with the energy difference $E_{01} = E_1 - E_0$ between the vibrational ground state $|\psi_0\rangle$ and the first excited state $|\psi_1\rangle$ of the Morse potential. The energy eigenvalues of the Morse potential is given by $E_n = [(n + 1/2) - (n + 1/2)^2/(2\lambda)] \hbar\omega_0$ for $n = 0, 1, \dots, [\lambda - 1/2]$, where $[x]$ denotes the largest integer smaller than x [47]. The cavity loss rate κ corresponds to an energy of 10 meV.

We first consider the single-molecule system, i.e., $N = 1$, for which a fully quantum mechanical calculation is

doable. Figure 2 compares the molecular nuclear dynamics and time evolution of the cavity photon number obtained by the TWA with those obtained by the fully quantum mechanical theory. The fully quantum mechanical result is obtained by solving the quantum master equation (3). The wavefunction of the ground state of the Morse potential is given by [47]

$$\begin{aligned} \psi_0(q) &= \sqrt{\frac{(2\lambda - 1)\alpha}{\Gamma(2\lambda)}} \left[2\lambda e^{-\alpha(q - q_e)} \right]^{\lambda - 1/2} \\ &\quad \times \exp \left[-\lambda e^{-\alpha(q - q_e)} \right]. \end{aligned} \quad (19)$$

A good agreement between the semiclassical TWA and fully quantum mechanical results is observed for the dynamics of both molecular nuclei and cavity photons.

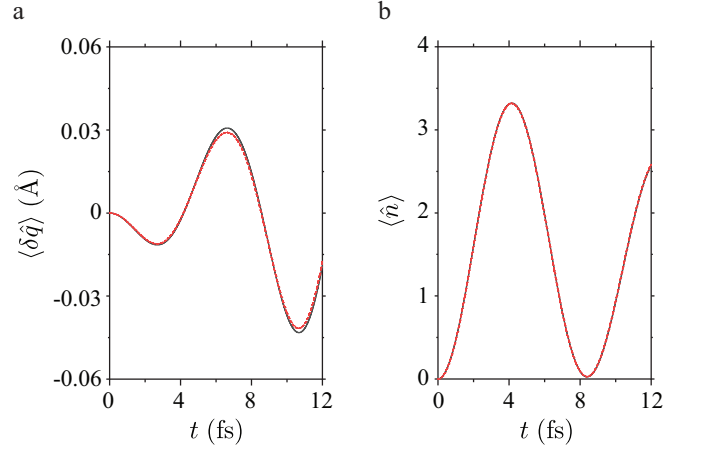


FIG. 2: Time evolutions of the expectation values of (a) the nuclear displacement operator $\delta \hat{q} = \hat{q} - q_0$ and (b) the cavity photon number operator $\hat{n} = \hat{a}^\dagger \hat{a}$ obtained by the semiclassical TWA (black, solid) and the fully quantum mechanical (red, dashed) theories. Here, the nuclear motion of a single diatomic molecule is coupled to an infrared cavity mode, and $q_0 = \langle \psi_0 | \hat{q} | \psi_0 \rangle$ is the initial expectation value of the nuclear distance operator \hat{q} for the vibrational ground state $|\psi_0\rangle$ of the Morse potential. The coupling strength is in the ultrastrong coupling regime such that both the molecular nuclei and cavity photons evolve with time, even if they are initially prepared in their ground states.

We next consider a system of $N = 30$ diatomic molecules, all aligned parallel to the polarization direction of the cavity mode. Here, the molecule-cavity collective coupling strength is kept constant, i.e., $g\sqrt{N}A\sqrt{\frac{\hbar}{M\omega_0}} = 0.1\hbar\omega_c$, implying that the coupling strength per molecule is reduced by a factor of $1/\sqrt{N}$ from the above case of the single-molecule system. Figure 3 shows the nuclear dynamics averaged over all the molecules inside the cavity. For comparison, the nuclear dynamics of the single-molecule system with constant collective coupling strength, i.e., $gA\sqrt{\frac{\hbar}{M\omega_0}} = 0.1\hbar\omega_c$, and that with constant coupling strength per molecule, i.e.,

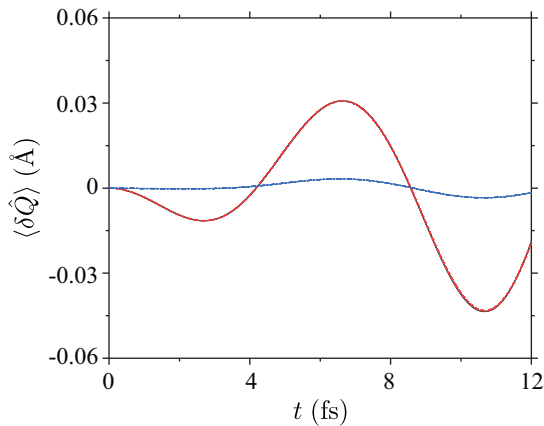


FIG. 3: Time evolution of the expectation value of the nuclear displacement operator averaged over all the molecules inside the cavity $\delta\hat{Q} = (1/N) \sum_{j=1}^N \hat{q}_j - q_0$ for a system of $N = 30$ diatomic molecules, all aligned parallel to the polarization direction of the cavity mode (black, solid). For comparison, the nuclear dynamics of the single-molecule system with constant collective coupling strength (red, dashed) and that with constant coupling strength per molecule (blue, dashed dot) are also shown.

$gA\sqrt{\frac{\hbar}{M\omega_0}} = 0.1\hbar\omega_c/\sqrt{N}$ are also shown in the figure. It is evident that the amplitude of the averaged nuclear dynamics does not decrease with the increasing number of molecules as long as the collective coupling strength is kept constant, and it is much larger than that of the single-molecule system with the same coupling strength per molecule. This is in sharp contrast to the case of linear systems such as a group of harmonic oscillators linearly coupled to an optical cavity mode. In a linear system, as long as the collective light-matter coupling strength is maintained at a constant level, the dynamic amplitude of the collective mode $\hat{q}_{\text{col}} = (1/\sqrt{N}) \sum_{j=1}^N \hat{q}_j$ is independent of the number of group members, and thus, the dynamic amplitude of an averaged observable such as $\hat{Q} = (1/N) \sum_{j=1}^N \hat{q}_j$ is strongly suppressed in large systems. Consequently, the collective effect observed here should be attributed to the molecular system's nonlinearity.

To investigate the dependence of the molecular nuclear dynamics on the cavity frequency, the first local maximum $Q_{\text{max}}^{(1)}$ in the time evolution of the expectation value $\langle \delta\hat{Q} \rangle$ of the averaged nuclear displacement operator is shown in Fig. 4 as a function of the detuning frequency $\delta\omega = \omega_c - E_{01}/\hbar$. Here, $\delta\hat{Q} = \hat{Q} - q_0$ with $q_0 = \langle \psi_0 | \hat{q} | \psi_0 \rangle$. It is clear that $Q_{\text{max}}^{(1)}$ is maximum when the cavity frequency is resonant with the energy difference between the vibrational ground state and the first excited state of the Morse potential. The dependence of the molecular nuclear dynamics on the cavity loss rate κ is also investigated. Figure 5 shows the nuclear dynamics for the rates corresponding to 1, 10, and 100 meV. The dynamic amplitude of the averaged nuclear displacement

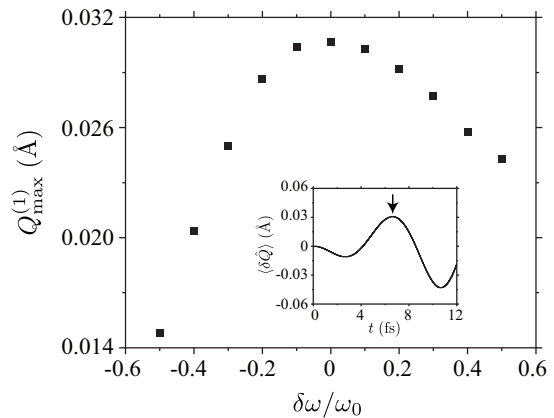


FIG. 4: The first local maximum $Q_{\text{max}}^{(1)}$ (indicated by the arrow in the inset) in the time evolution of the expectation value $\langle \delta\hat{Q} \rangle$ of the averaged nuclear displacement operator as a function of the detuning frequency $\delta\omega = \omega_c - E_{01}/\hbar$ normalized by ω_0 .

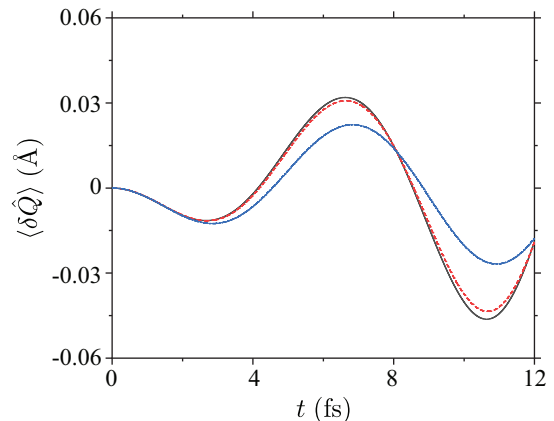


FIG. 5: Time evolutions of the expectation value $\langle \delta\hat{Q} \rangle$ of the averaged nuclear displacement operator for different values of the cavity loss rates κ corresponding to 1 meV (black, solid), 10 meV (red, dashed), and 100 meV (blue, dashed dot).

decreases with the increasing cavity loss rate as a result of the energy dissipation.

Finally, we investigate the nuclear dynamics in a system of molecules with random orientations strongly coupled to an optical cavity mode. The numerical calculations below consider a system of N diatomic molecules whose orientations are distributed evenly in the angular range of $0 \leq \theta \leq \pi$, i.e., $\theta_j = (j-1)\pi/(N-1)$ ($j = 1, \dots, N$). Here, θ_j is the angle between the direction of the j th molecule and the polarization direction of the cavity mode. As the molecule-cavity coupling g_j for the j th molecule is proportional to $\cos\theta_j$, its sign changes as the angle crosses $\pi/2$. Figure 6a shows the time evolutions of the expectation value of the nuclear displacement operator averaged over all the molecules $\delta\hat{Q} = (1/N) \sum_{j=1}^N \hat{q}_j - q_0$ for systems with varying numbers of molecules. It can be seen that $\langle \delta\hat{Q} \rangle$ for a system of many

molecules with random orientations is small compared to that for the single-molecule system with constant collective coupling strength. This is due to the dependence of the sign of the molecule-cavity coupling on the molecule's orientation. For example, in a system of two diatomic molecules with opposite directions, we have $g_2 = -g_1$. The cavity mode then only effectively couples to the nuclear motion's antisymmetric mode $\hat{Q}_{\text{as}} = (\hat{q}_1 - \hat{q}_2)/\sqrt{2}$ rather than the symmetric mode $\hat{Q}_{\text{s}} = (\hat{q}_1 + \hat{q}_2)/\sqrt{2}$. As a result, as long as such an observable that is a linear function of \hat{Q}_{s} as the averaged nuclear displacement is considered, a small dynamic amplitude should be expected. However, a larger dynamic amplitude can be observed for an observable that is a nonlinear function of \hat{Q}_{s} . Figure 6b shows the time evolution of the square root of the averaged variation of the nuclear displacement defined by $\delta Q_{\text{var}}(t) = \sqrt{\langle \hat{Q}_{\text{var}} \rangle(t) - \langle \hat{Q}_{\text{var}} \rangle(t=0)}$, where $\hat{Q}_{\text{var}} = (1/N) \sum_{j=1}^N (\hat{q}_j - q_0)^2$. It is evident that the dynamic amplitude of δQ_{var} for a system of many molecules with different orientations is smaller than that for the single-molecule system with constant collective coupling strength by a factor that is comparable to the reduction of the averaged coupling strength due to random orientations $\cos^2 \theta_j \simeq 1/2$. Moreover, unlike the case of linear systems such as a group of harmonic oscillators linearly coupled to an optical cavity mode, the dynamic amplitude of δQ_{var} does not decrease with the increasing number of molecules. Consequently, for a system of many molecules with random orientations, the collective effect of vibration-polariton formation on the molecular nuclear dynamics can be observed if the system and the observables are nonlinear.

Conclusion– We have developed the semiclassical TWA theory of molecular-vibration-polariton dynamics that is tractable in large molecular systems while simultaneously capturing the quantum character of photons in the optical cavity. The theory was then applied to investigate the nuclear dynamics of a system of diatomic molecules with a ground-state Morse potential and a nonlinear electric dipole moment strongly coupled to an infrared optical cavity mode in the ultrastrong coupling regime. For a system of many molecules aligned parallel to the polarization direction of the cavity mode, the collective effect of vibration-polariton formation manifested itself as the non-decreasing dynamic amplitude of the averaged nuclear displacement with the increasing number of molecules, provided that the collective coupling strength

is kept constant. The resonance effect of molecular-vibration-polariton formation was also observed. For a system of many molecules with random orientations, the collective effect of molecular-vibration-polariton dynamics persists if the system and the observables are nonlinear. The next step is to develop the TWA theory for the molecular-exciton-polariton dynamics, by which various interesting phenomena including, for example, the effect of polaron decoupling [50–53], super-reaction [54], Bose enhancement of excitation-energy transport [55],

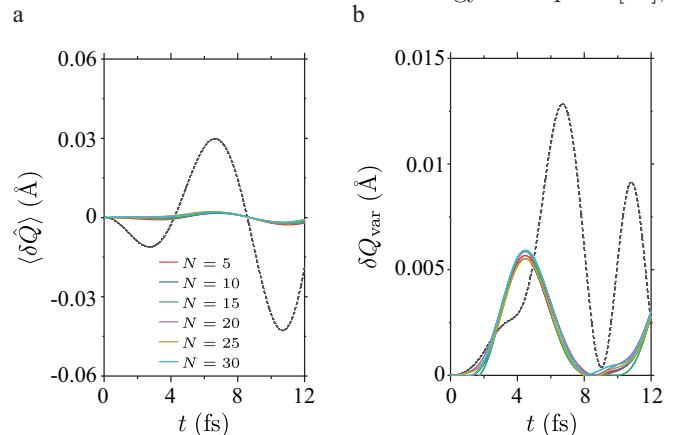


FIG. 6: Time evolutions of (a) the expectation value $\langle \delta \hat{Q} \rangle$ of the averaged nuclear displacement operator and (b) the square root of the averaged variation of the nuclear displacement δQ_{var} whose definition is given in the main text. The molecular orientations are distributed evenly in space. The number of molecules varies $N = 5, 10, 15, 20, 25, 30$ (indicated by the colors) while the collective coupling strength is kept constant. The nuclear dynamics of the single-molecule system with constant collective coupling strength (black, dashed) are shown in both (a) and (b) for comparison.

and photon-coupled electron spin dynamics [56], can be quantitatively studied in large molecular systems.

Acknowledgments

N. T. Phuc would like to thank Pham Quang Trung for fruitful discussion on numerical calculations. The computations were performed using Research Center for Computational Science, Okazaki, Japan.

[1] Nagarajan, K.; Thomas, A.; Ebbesen, T. W. Chemistry under Vibrational Strong Coupling. *J. Am. Chem. Soc.* **2021**, *143*, 16877–16889.
 [2] Simpkins, B. S.; Dunkelberger, A. D.; Vurgaftman, I. Control, Modulation, and Analytical Descriptions of Vibrational Strong Coupling. *Chem. Rev.* **2023**, *123*, 5020–5048.

[3] Hirai, K.; Hutchison, J. A.; Uji-i, H. Molecular Chemistry in Cavity Strong Coupling. *Chem. Rev.* **2023**, *123*, 8099–8126.
 [4] Thomas, A.; Jayachandran, A.; Lethuillier-Karl, L.; Vergauwe, R. M. A.; Nagarajan, K.; Devaux, E.; Genet, C.; Moran, J.; Ebbesen, T. W. Ground-State Chemical Reactivity under Vibrational Coupling to the Vacuum

- Electromagnetic Field. *Angew. Chem. Int. Ed.* **2016**, *55*, 11462–11466.
- [5] Vergauwe, R. M. A.; Thomas, A.; Nagarajan, K.; Shalabney, A.; George, J.; Chervy, T.; Seidel, M.; Devaux, E.; Torbeev, V.; Ebbesen, T. W. Modification of Enzyme Activity by Vibrational Strong Coupling of Water. *Angew. Chem. Int. Ed.* **2019**, *58*, 15324–15328.
- [6] Lather, J.; Bhatta, P.; Thomas, A.; Ebbesen, T. W.; George, J. Cavity Catalysis by Cooperative Vibrational Strong Coupling of Reactant and Solvent Molecules. *Angew. Chem. Int. Ed.* **2019**, *58*, 10635–10638.
- [7] Hirai, K.; Takeda, R.; Hutchison, J. A.; Uji-i, H. Modulation of Prins Cyclization by Vibrational Strong Coupling. *Angew. Chem. Int. Ed.* **2020**, *59*, 5332–5335.
- [8] Pang, Y.; Thomas, A.; Nagarajan, K.; Vergauwe, R. M. A.; Joseph, K.; Patrahau, B.; Wang, K.; Genet, C.; Ebbesen, T. W. On the Role of Symmetry in Vibrational Strong Coupling: The Case of Charge-Transfer Complexation. *Angew. Chem. Int. Ed.* **2020**, *59*, 10436–10440.
- [9] Sau, A.; Nagarajan, K.; Patrahau, B.; Lethuillier-Karl, L.; Vergauwe, R. M. A.; Thomas, A.; Moran, J.; Genet, C.; Ebbesen, T. W. Modifying Woodward-Hoffmann Stereoselectivity under Vibrational Strong Coupling. *Angew. Chem. Int. Ed.* **2021**, *60*, 5712–5717.
- [10] Lather, J.; George, J. Improving Enzyme Catalytic Efficiency by Co-Operative Vibrational Strong Coupling of Water. *J. Phys. Chem. Lett.* **2021**, *12*, 379–384.
- [11] Thomas, A.; Lethuillier-Karl, L.; Nagarajan, K.; Vergauwe, R. M. A.; George, J.; Chervy, T.; Shalabney, A.; Devaux, E.; Genet, C.; Moran, J.; Ebbesen, T. W. Tilting a ground-state reactivity landscape by vibrational strong coupling. *Science* **2019**, *363*, 615–619.
- [12] Joseph, K.; Kushida, S.; Smarsly, E.; Ihiwakrim, D.; Thomas, A.; Paravicini-Bagliani, G. L.; Nagarajan, K.; Vergauwe, R.; Devaux, E.; Ersen, O.; Bunz, U. H. F.; Ebbesen, T. W. Supramolecular Assembly of Conjugated Polymers under Vibrational Strong Coupling. *Angew. Chem. Int. Ed.* **2021**, *60*, 19665–19670.
- [13] Hirai, K.; Ishikawa, H.; Chervy, T.; Hutchison, J. A.; Uji-i, H. Selective Crystallization Via Vibrational Strong Coupling. *Chem. Sci.* **2021**, *12*, 11986.
- [14] Xiang, B.; Ribeiro, R. F.; Du, M.; Chen, L.; Yang, Z.; Wang, J.; Yuen-Zhou, J.; Xiong, W. Intermolecular Vibrational Energy Transfer Enabled by Microcavity Strong Light-Matter Coupling. *Science* **2020**, *368*, 665–667.
- [15] Thomas, A.; Devaux, E.; Nagarajan, K.; Rogez, G.; Seidel, M.; Richard, F.; Genet, C.; Drillon, M.; Ebbesen, T. W. Large Enhancement of Ferromagnetism under a Collective Strong Coupling of YBCO Nanoparticles. *Nano Lett.* **2021**, *21*, 4365–4370.
- [16] Thomas, A.; Devaux, E.; Nagarajan, K.; Chervy, T.; Seidel, M.; Hagenmuller, D.; Schutz, S.; Schachenmayer, J.; Genet, C.; Pupillo, G.; Ebbesen, T. W. Exploring Superconductivity under Strong Coupling with the Vacuum Electromagnetic Field. *arXiv Preprint* **2019**, No. arXiv:1911.01459v2[cond-mat.supr-con].
- [17] Galego, J.; Climent, C.; Garcia-Vidal, F. J.; Feist, J. Cavity Casimir-Polder forces and their effects in ground state chemical reactivity. *Phys. Rev. X* **2019**, *9*, 021057 (2019).
- [18] Campos-Gonzalez-Angulo, J. A.; Ribeiro, R. F.; Yuen-Zhou, J. Resonant catalysis of thermally-activated chemical reactions with vibrational polaritons. *Nat. Comm.* **2019**, *10*, 4685.
- [19] Phuc, N. T.; Trung, P. Q.; Ishizaki, A. Controlling the nonadiabatic electron-transfer reaction rate through molecular-vibration polaritons in the ultrastrong coupling regime. *Sci. Rep.* **2020**, *10*, 7318.
- [20] Li, T. E.; Subotnik, J. E.; Nitzan, A. Cavity molecular dynamics simulations of liquid water under vibrational ultrastrong coupling. *Proc. Natl. Acad. Sci. U.S.A.* **2020**, *117*, 18324–18331.
- [21] Li, X.; Mandal, A.; Huo, P. Cavity frequency-dependent theory for vibrational polariton chemistry. *Nat. Comm.* **2021**, *12*, 1315.
- [22] Schafer, C.; Flick, J.; Ronca, E.; Narang, P.; Rubio, A. Shining Light on the Microscopic Resonant Mechanism Responsible for Cavity-Mediated Chemical Reactivity. *Nat. Commun.* **2022**, *13*, 7817.
- [23] Du, M.; Yuen-Zhou, J. Catalysis by Dark States in Vibropolaritonic Chemistry. *Phys. Rev. Lett.* **2022**, *128*, 96001.
- [24] Riso, R. R.; Haugland, T. S.; Ronca, E.; Koch, H. Molecular Orbital Theory in Cavity QED Environments. *Nat. Commun.* **2022**, *13*, 1368.
- [25] Sun, J.; Vendrell, O. Suppression and enhancement of thermal chemical rates in a cavity. *J. Phys. Chem. Lett.* **2022**, *13*, 4441–4446.
- [26] Wang, D. S.; Neuman, T.; Yelin, S. F.; Flick, J. Cavity-modified unimolecular dissociation reactions via intramolecular vibrational energy redistribution. *J. Phys. Chem. Lett.* **2022**, *13*, 3317–3324.
- [27] Wang, D. S.; Flick, J.; Yelin, S. F. Chemical reactivity under collective vibrational strong coupling. *J. Chem. Phys.* **2022**, *157*, 224304.
- [28] Lindoy, L. P.; Mandal, A.; Reichman, D. R. Quantum dynamical effects of vibrational strong coupling in chemical reactivity. *Nat. Commun.* **2023**, *14*, 2733.
- [29] Wang, D. S.; Yelin, S. F. A Roadmap Toward the Theory of Vibrational Polariton Chemistry. *ACS Photonics* **2021**, *8*, 2818–2826.
- [30] Fregoni, J.; Garcia-Vidal, F. J.; Feist, J. Theoretical Challenges in Polaritonic Chemistry. *ACS Photonics* **2022**, *9*, 1096–1107.
- [31] Campos-Gonzalez-Angulo, J. A.; Poh, Y. R.; Du, M.; Yuen-Zhou, J. Swinging between shine and shadow: Theoretical advances on thermally activated vibropolaritonic chemistry. *J. Chem. Phys.* **2023**, *158*, 230901.
- [32] Mandal, A.; Taylor, M. A. D.; Weight, B. M.; Koessler, E. R.; Li, X.; Huo, P. Theoretical Advances in Polariton Chemistry and Molecular Cavity Quantum Electrodynamics. *Chem. Rev.* **2023**, *123*, 9786–9879.
- [33] Moyal, J. Quantum mechanics as a statistical theory. *Math. Proc. Camb. Philos. Soc.* **1949**, *45*, 99–124.
- [34] Hillery, M.; O’Connell, R. F.; Scully, M. O.; Wigner, E. P. Distribution functions in physics: Fundamentals. *Phys. Rep.* **1984**, *106*, 121–167.
- [35] Polkovnikov, A. Phase space representation of quantum dynamics. *Ann. Phys.* **2010** *325*, 1790–1852.
- [36] Walls, D.; Milburn, G. *Quantum Optics*; Springer-Verlag, Berlin, 1994.
- [37] Blakie, P. B.; Bradley, A. S.; Davis, M. J.; Ballagh, R. J.; Gardiner, C. W. Dynamics and statistical mechanics of ultra-cold Bose gases using c-field techniques. *Adv. Phys.* **2008**, *57*, 363–455.
- [38] Zurek, W. H. Decoherence, einselection, and the quantum origins of the classical. *Rev. Mod. Phys.* **2003**, *75*,

- 715–775.
- [39] Mondal, S.; Wang, D. S.; Keshavamurthy, S. Dissociation dynamics of a diatomic molecule in an optical cavity. *J. Chem. Phys.* **2023**, *157*, 244109.
- [40] Kockum, A. F.; Miranowicz, A.; Liberato, S. D.; Savasta, S.; Nori, F. Ultrastrong Coupling between Light and Matter. *Nat. Rev. Phys.* **2019**, *1*, 19–40.
- [41] Cohen-Tannoudji, C.; Dupont-Roc, J.; Grynberg, G. *Photons and Atoms: Introduction to Quantum Electrodynamics*; Wiley: Weinheim, 1997.
- [42] Power, E. A.; Zienau, S. Coulomb Gauge in Non-Relativistic Quantum Electro-Dynamics and the Shape of Spectral Lines. *Philos. Trans. R. Soc. A* **1959**, *251*, 427–454.
- [43] Woolley, R. G. A Reformulation of Molecular Quantum Electrodynamics. *J. Phys. B: At. Mol. Phys.* **1974**, *7*, 488–499.
- [44] Rokaj, V.; Welakuh, D. M.; Ruggenthaler, M.; Rubio, A. Light-Matter Interaction in the Long-wavelength Limit: No Ground-State without Dipole Self-Energy. *J. Phys. B: At. Mol. Opt. Phys.* **2018**, *51*, 034005.
- [45] Lindblad, G. On the Generators of Quantum Dynamical Semigroups. *Comm. Math. Phys.* **1976**, *48*, 119–130.
- [46] Carmichael, H. J. *Statistical Methods in Quantum Optics 1: Master Equations and Fokker-Planck Equations*; Springer-Verlag, Berlin, 1999.
- [47] Dahl, J. P.; Springborg, M. The Morse oscillator in position space, momentum space, and phase space. *J. Chem. Phys.* **1988**, *88*, 4535.
- [48] Gilat, A.; Subramaniam, V. *Numerical Methods for Engineers and Scientists: An Introduction with Applications Using MATLAB*; John Wiley & Sons, Inc., NJ, 2011.
- [49] Tuckerman, M. E. *Statistical Mechanics: Theory and Molecular Simulation*; Oxford University Press, New York, 2010.
- [50] Spano, F. C. Optical microcavities enhance the exciton coherence length and eliminate vibronic coupling in J-aggregates. *J. Chem. Phys.* **2015**, *142*, 184707.
- [51] Herrera, F.; Spano, F. C. Cavity-Controlled Chemistry in Molecular Ensembles. *Phys. Rev. Lett.* **2016**, *116*, 238301.
- [52] Phuc, N. T.; Ishizaki, A. Precise determination of excitation energies in condensed-phase molecular systems based on exciton-polariton measurements. *Phys. Rev. Res.* **2019**, *1*, 033019.
- [53] Takahashi, S.; Watanabe, K. Decoupling from a thermal bath via molecular polariton formation. *J. Phys. Chem. Lett.* **2020**, *11*, 1349–1356.
- [54] Phuc, N. T. Super-reaction: The collective enhancement of a reaction rate by molecular polaritons in the presence of energy fluctuations. *J. Chem. Phys.* **2021**, *155*, 014308.
- [55] Phuc, N. T. Bose enhancement of excitation-energy transfer with molecular-exciton-polariton condensates. *J. Chem. Phys.* **2022**, *156*, 234301.
- [56] Phuc, N. T. Chiral-induced spin selectivity in photon-coupled achiral matters. *J. Phys. Chem. Lett.* **2023**, *14*, 1626–1632.